SLAC–PUB–6470
OREXP-94-1
March 1994
(E/T)

Precise Measurement of the Left-Right Cross Section Asymmetry in Z Boson Production by Electron-Positron Collisions*

The SLD Collaboration
Stanford Linear Accelerator Center
Stanford University, Stanford, California 94309

represented by

Raymond E. Frey
University of Oregon, Eugene, Oregon 97403

ABSTRACT

A precise measurement of the left-right cross section asymmetry (A_{LR}) for Z boson production by e^+e^- collisions has been attained at the Slac Linear Collider with the SLD detector. We describe this measurement for the 1993 data run, emphasizing the significant improvements in polarized beam operation which took place for this run, where the luminosity-weighted electron beam polarization averaged $62.6 \pm 1.2\%$. Preliminary 1993 results for A_{LR} are presented. When combined with the (less precise) 1992 result, the preliminary result for the effective weak mixing angle is $\sin^2 \theta_W^{\text{eff}} = 0.2290 \pm 0.0010$.

Presented at the SLAC Summer Institute on Particle Physics: Spin Structure in High Energy Processes Stanford, CA, July 26 - August 6, 1993

*Work supported by Dept. of Energy contracts DE-FG06-85ER40224 and DE-AC03-76SF00515.

1 Introduction

The first run with longitudinally polarized electron beam at the SLAC Linear Collider (SLC) took place during 1992. The average polarization for that run was measured to be $22.4 \pm 0.7\%$. During the best running the SLD experiment recorded about 1000 Z events per week, and a total sample of 10,224 events were used to produce the first result[1] for the left-right Z boson cross section asymmetry (A_{LR}) by e^+e^- collisions. The precision of that result was completely dominated by the statistical error of 44% in A_{LR}. By a combination of improved luminosity and much greater polarization, the precision of the result for the 1993 run has improved by a factor 10. Roughly speaking, the SLC luminosity improved by a factor 2 in 1993 due to many factors, most notably the advent of flat beam running; the polarization improved by slightly less than a factor of 3, due to the use of strained lattice photocathodes. These improvements are discussed in some detail in Section 2.

The left-right asymmetry is defined as,

$$A_{LR} \equiv (\sigma_L - \sigma_R) / (\sigma_L + \sigma_R), \tag{1}$$

where σ_L and σ_R are the e^+e^- production cross sections for Z bosons (at the Z pole) with left-handed and right-handed electrons, respectively. The properties of A_{LR} are discussed in detail elsewhere.[2,3] To leading order, the Standard Model predicts that this quantity depends upon the vector (v_e) and axial-vector (a_e) couplings of the Z boson to the electron current,

$$A_{LR} = \frac{2v_e a_e}{v_e^2 + a_e^2} = \frac{2\left[1 - 4\sin^2\theta_W^{\rm eff}\right]}{1 + \left[1 - 4\sin^2\theta_W^{\rm eff}\right]^2} \tag{2}$$

We retain the tree-level relations between the couplings and the electroweak mixing parameter to compare with the experimental measurement of A_{LR}, effectively including higher-order corrections in $\sin^2\theta_W^{\rm eff}$ (as well as a_e and v_e). This effective electroweak mixing parameter is then defined by $\sin^2\theta_W^{\rm eff} \equiv (1 - v_e/a_e)/4$. This convention is particularly useful for the measurement of the electroweak asymmetries at the Z resonance, and we follow the LEP Collaborations[4] in doing so.

A_{LR} has a number of nice properties. First, it is a sensitive function of $\sin^2\theta_W^{\rm eff}$, with $\delta\sin^2\theta_W^{\rm eff} \approx \delta A_{LR}/7.8$. It is large ($> 0.1$). It is relatively insensitive to energy. Finally, A_{LR} does not depend upon the couplings of the Z to its final states.

Hence, all visible Z decay modes can in principle be used in the measurement. In practice, the e^+e^- final state is discarded by SLD due to its large zero-asymmetry contribution from photon exchange. Also, for the calorimetric event selection used in the A_{LR} analysis, SLD does not select $\mu^+\mu^-$ final states, and is not very efficient in selecting $\tau^+\tau^-$ events. However, this still leaves about 3/4 of the total Z cross section which can be used for A_{LR}. This represents a tremendous statistical advantage over Z asymmetry measurements which rely on a single final state.

The experimental aspects of the A_{LR} measurement are also rather unique. The SLD detector is not required to identify specific final states, except to discard e^+e^- events. The switching between left and right-hand polarization states is done randomly at 120 Hz, which, in principle, makes the integrated luminosity for left and right-handed running identical. In this case, the definition of Eqn. 1 becomes

$$A_m = \frac{N_L - N_R}{N_L + N_R} \tag{3}$$

The experimental difficulty is dominated by the measurement of the electron beam polarization, $\mathcal{P}_e$. For a partially polarized beam the experimental determination of A_{LR} is essentially $A_{LR} = A_m/\mathcal{P}_e$. Small corrections to this formulation are discussed in Section 5. In this approximation, the A_{LR} measurement error is

$$\delta A_{LR} = \Big[\frac{1}{N_Z \mathcal{P}_e^2} + A_{LR}^2\Big(\frac{\delta\mathcal{P}_e}{\mathcal{P}_e}\Big)^2\Big]^{1/2}, \tag{4}$$

where $N_Z = N_L + N_R$ is the total number of events and $\delta\mathcal{P}_e$ is the error in the polarization measurement. We see immediately from this that a large polarization is critical, and that the relative error on the polarization measurement needs to be a few percent or less.

2 The SLC and Polarized Beam

A convenient expression for the luminosity of a linear e^+e^- collider is

$$\mathcal{L} = \frac{N^+N^-fH_D}{4\pi(\beta_x^*\beta_y^*\epsilon_x\epsilon_y)^{1/2}} \tag{5}$$

Here N^+ and N^- are the colliding e^+ and e^- bunch populations, and f is the frequency of collision (120 Hz for the SLC). β^* is essentially the focal length at the e^+e^- interaction point (IP), and ϵ is the beam emittance. H_D is an enhancement

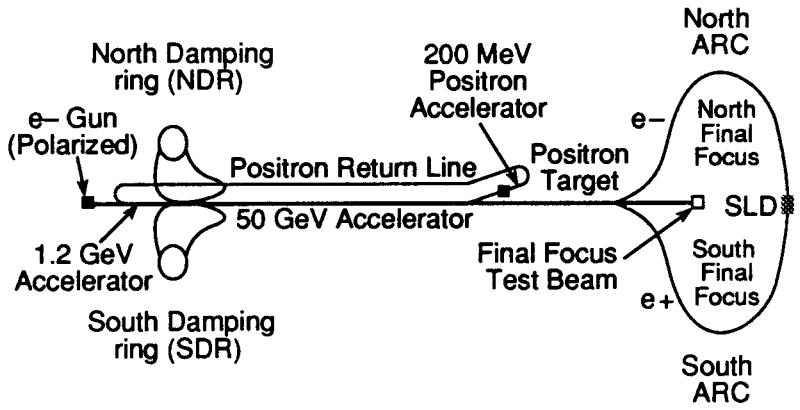

Figure 1: Simplified schematic of the SLC.

factor due to the additional contraction of one bunch as it passes through the intense collective electromagnetic field of the other bunch. This factor is one for small fields. It was estimated to be as large as 1.1–1.2 during the best 1993 running, but has yet to be directly measured.

In describing the operation of the SLC with polarized beam, we emphasize below changes in SLC operation for 1993 which resulted in major improvements for the experimental program. There are a number of excellent descriptions[3] of other aspects of polarized SLC operation which are largely unchanged. The most dramatic changes for the 1993 run included the use of strained-lattice cathodes at the SLC source, which gave a large increase in electron beam polarization (from 22% to 63%), and the advent of flat beam operation, which gave higher luminosity (by a factor ≈ 2). Figure 1 gives the overall SLC layout.

2.1 The Polarized Electron Source

During the initial run with polarized beam in 1992, the polarization was mostly limited by the "thick" GaAs photocathode at the electron source, resulting in an average polarization at the e^+e^- IP of 22.4%. Meanwhile, an interesting program of R&D on strained-lattice photocathodes indicated[5] that much higher polarization was possible. These results are summarized in Fig. 2. In unstrained GaAs, the theoretical maximum polarization of the emitted electrons is 50%, owing to the degeneracy of two competing transitions. The 1993 strained lattice consists of a $GaAs_{1-x}P_x$ ($x = 0.24$) substrate of thickness 2.5 μm with an epitaxial layer

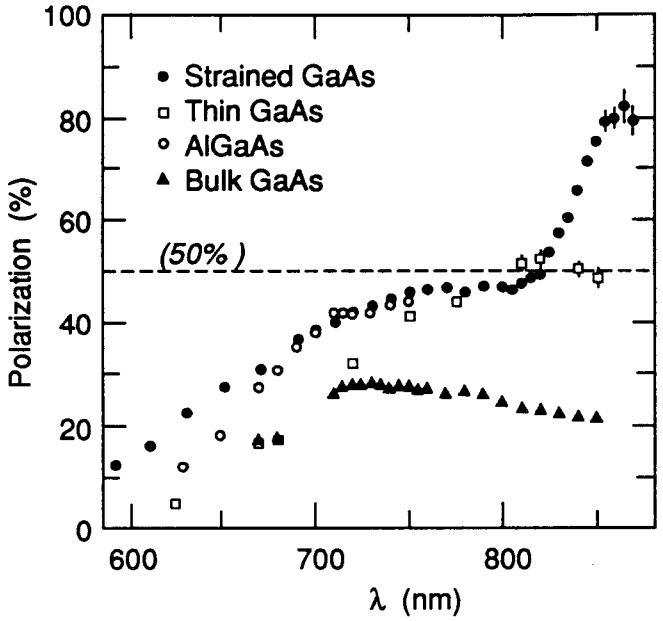

Figure 2: Summary of photocathode R&D.

of GaAs of thickness 0.1–0.3 μm. This alters the lattice spacing over a significant depth in the photocathode, hence removing the transition degeneracy. As with previous photocathodes, approximately one atomic layer of cesium and fluorine applied to the cathode surface substantially increases the quantum efficiency (5–15%), thereby making the devices practical for SLC operation. With the GaAs degeneracy removed, a Ti-saphire laser[6] operating at 865 nm excites the lower-energy transition. Figure 3 shows the measured polarization at the IP over the course of the 1993 run. Each point in the plot represents the measured polarization associated with a Z event recorded by SLD. At about day 100, the laser wavelength was changed from 850 nm to 865 nm, thus maximizing the preferred GaAs transition. The variation of the measurements over time represents correlations with changes in SLC operation, generally either due to re-coating of the source photocathode or to a re-tuning of the arc orbit, as described below.

2.2 Beam and Spin Transport

Upon arriving at the electron damping ring, the 1.2 GeV longitudinally polarized beam must be spin-rotated to the vertical, thus avoiding depolarization during the damping process. In the presence of a uniform magnetic field transverse to the

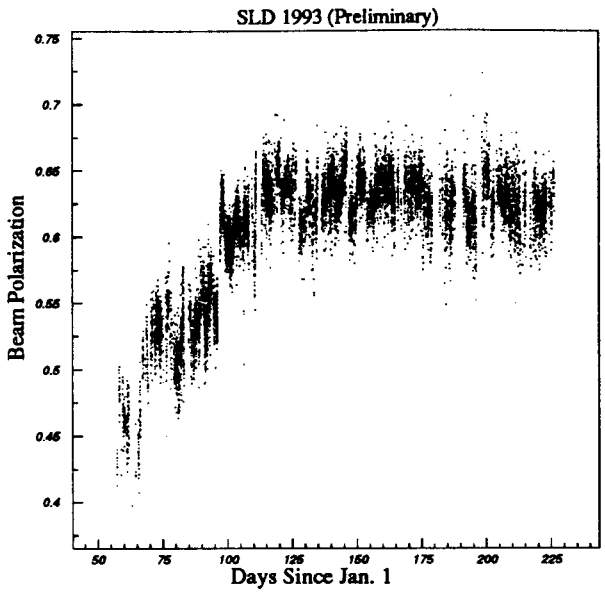

Figure 3: Measured polarization versus days from the start of the 1993 run for each recorded Z event.

plane containing the electron spin and momentum vectors, high-energy electrons will undergo 90° of spin rotation in that plane for every 32.8° of momentum rotation in the plane. In redirecting the electrons from the Linac to the North Damping Ring (NDR), the beam is rotated by $5 \times 32.8°$. This is illustrated in Fig. 4. The transverse spins are then rotated to the vertical by a 6.3 T-m superconducting solenoid in the Linac-to-Ring (LTR) line. During the 1992 polarized run, the beam exiting the NDR was made to pass through a pair of solenoids in the Ring-to-Linac (RTL) line, thus rotating the electron spin back to (near) longitudinal in order to ultimately achieve longitudinal polarization at the IP. However, for the 1993 run the RTL solenoids were not energized, as discussed below.

In the absence of chromatic effects, the beam spot size at focus is, by Eqn. 5, proportional to the square root of the product of the beam emittances, ϵ_x and ϵ_y. It had long been thought that the IP spot size could possibly be reduced by producing "flat" (*i.e.* elliptical) beam in the damping rings, something which damping rings are naturally inclined to do well. Prior to 1992 it was thought that polarized beam transport was incompatible with flat beams. A solenoidal field will introduce x-y coupling of the beam phase space due to the beam betatron motion. Therefore, the RTL solenoid, necessary to produce longitudinal

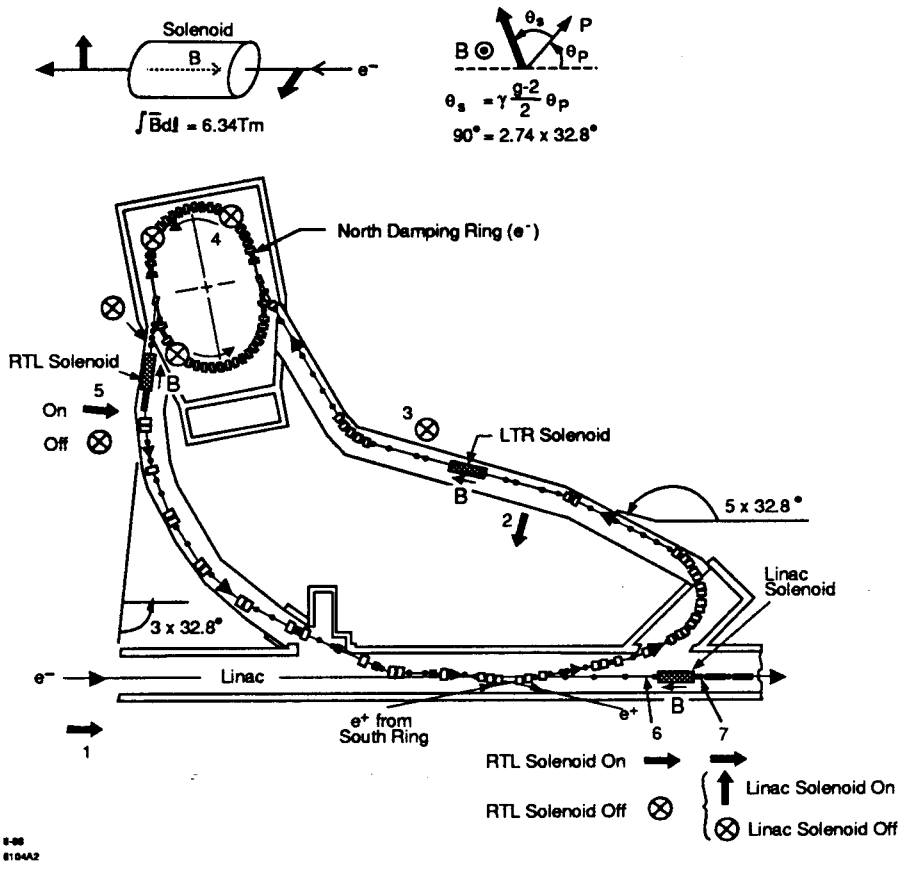

Figure 4: North (electron) Damping Ring beam transport. The numbers indicate the sequence of events and the arrows indicate the polarization direction. Note that for the 1993 run the RTL solenoids were off.

polarization, would ruin the flat beams.

Flat-beam running with polarized beam was only made possible by "spin bumps", a property of the SLC arcs discovered[7] during the first run with polarized beam in 1992. It was found that the polarization at the IP was strongly affected by the position of the electron beam launch into the arc. Longitudinally polarized electrons launched into the North Arc undergo $g-2$ precession in the arc bending fields. Normally, the resulting IP polarization would be very insensitive to the arc launch details. However, as it turns out, the spin precession frequency in the arc is almost exactly equal to the arc betatron oscillation frequency. (Each of the 23 arc achromats produces 1085° of spin precession and 1080° of betatron oscillation.) This means that spin precession in a non-bend plane can accumulate during the focussing-defocussing process by an amount which depends on arc

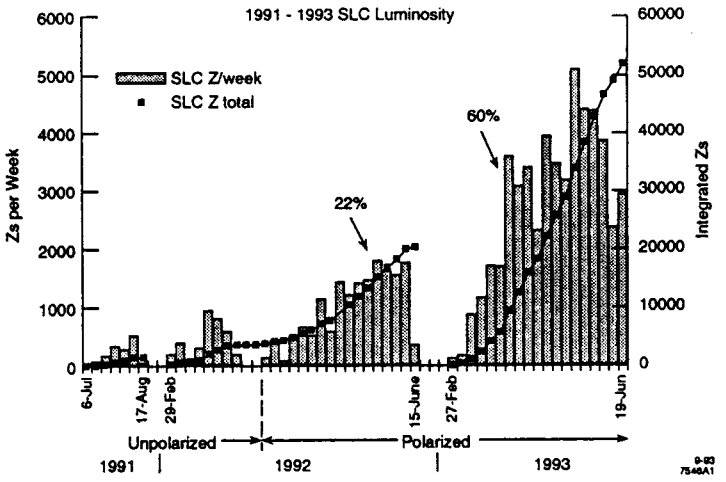

Figure 5: SLC luminosity performance for 1991–93. The last two months of the 1993 run are not included.

launch position. In practice, a vertically polarized beam at the end of the Linac can be made longitudinal at the IP by a pair of large betatron oscillations in the North Arc. This was standard practice for the 1993 run.

SLD running with flat beams began near the start of the 1993 run, and was largely responsible for the increase of ≈ 2 in instantaneous luminosity over the best 1992 running. This can be seen in Fig. 5, which indicates how the SLC luminosity has evolved since 1991. Two notes concerning this figure. It gives integrated luminosity in terms of number of Z events *delivered* by the SLC (one Z is defined as 30 nb^{-1}), whereas the actual number of events recorded by the SLD detector is reduced, both by data-taking efficiency (typically $\sim 90\%$) and by the fact that (head-on) collisions are not produced on every SLC pulse. Also, the plot does not include the last two months of the run. By the end of the run the number of Z events recorded by SLD exceeded 5×10^4.

The maximum luminosity in 1993 was about 5×10^{29} $\text{cm}^{-2}\text{s}^{-1}$. The emittance ratio exiting the damping rings was $\epsilon_x/\epsilon_y = 10$. The beam emittance was not allowed to substantially grow to the IP, itself a formidable task due to the presence of potentially large wake field effects. The beams are focussed at the IP to spot sizes with the expected 3/1 aspect ratio. Individual values during good conditions were $\sigma_x = 2.5\,\mu\text{m}$ and $\sigma_x = 0.8\,\mu\text{m}$. This is illustrated in Fig. 6, which indicates the evolution of the IP spot sizes, including future prospects which are discussed further in Section 5.

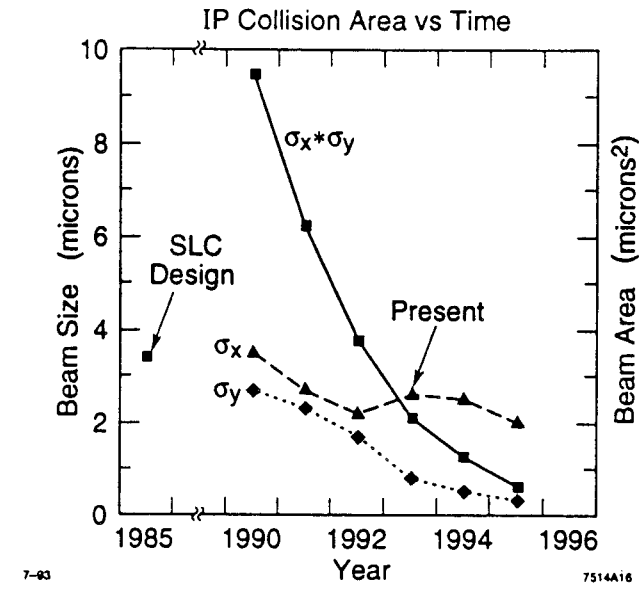

Figure 6: Evolution of SLC interaction point beam spot size.

We turn now to a troublesome spin transport issue which arose in 1993, but is now fully understood and will be not be an issue for the foreseeable future. The typical energy spread of the SLC beam is $\Delta E/E \approx 0.2\%$. Since the net spin precession in the North Arc is proportional to energy, one expects each beam energy component to have a slightly different degree of longitudinal polarization at the IP. For the gaussian core of the beam, the net reduction in polarization at the IP due to this "spin diffusion" is small ($< 1\%$) and is in itself of little consequence.

Now, in principle, the focussing of the beams at the IP can map each beam-energy component to a different effective point of focus, resulting in a correlation between transverse position at the IP and energy, or equivalently between position and polarization. Even though the present SLC Final Focus optics includes chromatic correction, the extremely small vertical emittance in 1993 allowed this position-energy correlation to become more significant, a result of third-order chromatic aberrations in the optics. Models have indicated that the vertical spot size at the IP indeed may have been limited by these higher order aberrations in 1993. Still, this would not be an experimental issue except that the polarization of those electrons which weight Z production at the IP can be different from the polarization of the entire electron beam, averaged over its full spatial extent. In the former case, the electron beam is sampled by its interaction probability to

make Z's via positrons; this is referred to as the luminosity-weighted polarization, $\mathcal{P}_e$. The latter case is relevant for the polarization measurement using Compton scattering, $\mathcal{P}_e^C$, as the spatial extent of the Compton laser beam is much larger than the electron beam, hence sampling all electrons with equal weight.

If the electron beam had only gaussian energy tails, the difference between $\mathcal{P}_e$ and $\mathcal{P}_e^C$ would be small ($< 0.2\%$) and readily modelled. However, the beam was observed to have a long low-energy tail extending to $\Delta E/E$ of about -1%. The correction for this effect has been addressed in the following way. First, the beam tail and optics were modelled, and it was found that the measured $\mathcal{P}_e^C$ agreed well with the amount of beam tail allowed to propagate to the IP, as determined by the position of a collimator at a low-dispersion point of the North Arc. The model can be confidently used to estimate the minimum possible difference between $\mathcal{P}_e$ and $\mathcal{P}_e^C$ by the constraint that it not predict a luminosity in excess of that observed. The maximum effect is conservatively given by the difference between the measured polarization at the end of the Linac and that at the IP. Assigning no *a priori* preference within this allowed range, the correction becomes

$$\mathcal{P}_e = (1.017 \pm 0.012)\mathcal{P}_e^C \tag{6}$$

The model alone, without further input, gives a similar correction of 1.019 ± 0.005.

For running beyond 1993 it is well understood how to remove the low-energy beam tail. The expected correction factor will be very small ($< 0.5\%$), and the error on the correction will become negligible.

3 Polarization Measurement

The primary measurement of the electron beam polarization is accomplished by measuring Compton scattering of polarized light with the polarized electrons. This is done in concert with normal SLC/SLD operation. For special runs, the electron beam at the end of the Linac can be diverted from the SLC arc to the PEP extraction line, where a polarization measurement based on Møller scattering is performed. The Compton and Møller polarimetry, in addition to a number of tests and consistency checks of the measurements, are briefly described below. Careful analysis of all aspects of polarization transport and measurement for the 1993 resulted in a fully consistent and well understood polarization measurement.

3.1 Compton Polarimetry

The overall layout of the Compton scattering measurement of the electron beam polarization is shown in Fig. 7. The measurement technique is not substantially changed from the 1992 run.[1,8] Longitudinally polarized photons of energy 2.33 eV, provided by 532 nm circularly polarized laser pulses from a frequency-doubled Nd:YAG laser, are brought into collision with the outgoing electron beam 33 m past the IP. The back-scattered Compton electrons, ranging in energy from 17.4 GeV to about 30 GeV, are detected by a multi-channel Cerenkov detector after being separated from the main electron beam by two dipole magnets which are the final bend magnets of the SLC Final Focus. At the face of the Cerenkov detector, the Compton electrons shower in a retractable 8 mm lead radiator. The Cerenkov gas is non-scintillating β-butylene at 1.0 atm. The Compton cross section can be written

$$\frac{d\sigma}{dE_s} = \frac{d\sigma_0}{dE_s}[1 + \mathcal{P}_\gamma \mathcal{P}_e^C A(E_s)]\,, \tag{7}$$

where E_s is the Compton-scattered electron energy, $\mathcal{P}_\gamma$ is the polarization of the laser photon beam, $\mathcal{P}_e^C$ is the electron beam polarization, and $A(E_s)$ is the Compton polarization asymmetry function. $A(E_s)$ is the asymmetry in the theoretical Compton cross section for the $J_z = \frac{3}{2}$ versus $\frac{1}{2}$ combinations of $e\gamma$. It also includes corrections of about 2% to account for the response of the Cerenkov detector. The maximum asymmetry occurs at the kinematic endpoint, $E_s = 17.4$ GeV, which corresponds to 180° electron scattering in the $e\gamma$ center-of-momentum frame. The Compton measurement is illustrated in Fig. 8 for the 1992 run. Each point represents the measured asymmetry in one of seven channels of the Cerenkov detector. E_s is given on the top of the plot, and the corresponding distance d from the unscattered electron beam is also shown. The Compton process itself gives fiducials which can be used to calibrate the Cerenkov detector. The kinematic endpoint can be precisely determined in the detetector. The detector can, in special runs, be translated across the endpoint to verify the single-channel response function. The distance between kinematic endpoint and zero-asymmetry point (25.2 GeV) is particularly well measured, and serves as a length-scale check of the detector and bend magnets. The measured asymmetry in each detector channel is equal to the combination $\mathcal{P}_\gamma \mathcal{P}_e^C A(E_s)$, where E_s corresponds to the mean energy for that channel. The curve in Fig. 8 is a fit to the theoretical asymmetry function, leaving the product $\mathcal{P}_\gamma \mathcal{P}_e^C$ as a free parameter measured by this procedure.

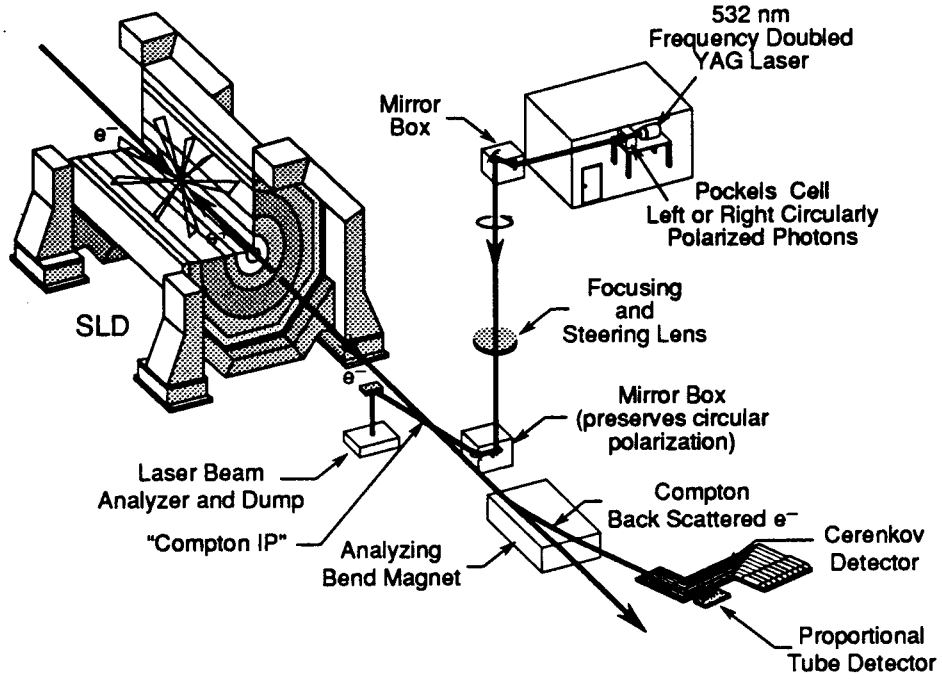

Figure 7: Schematic of the Compton scattering polarization measurement technique.

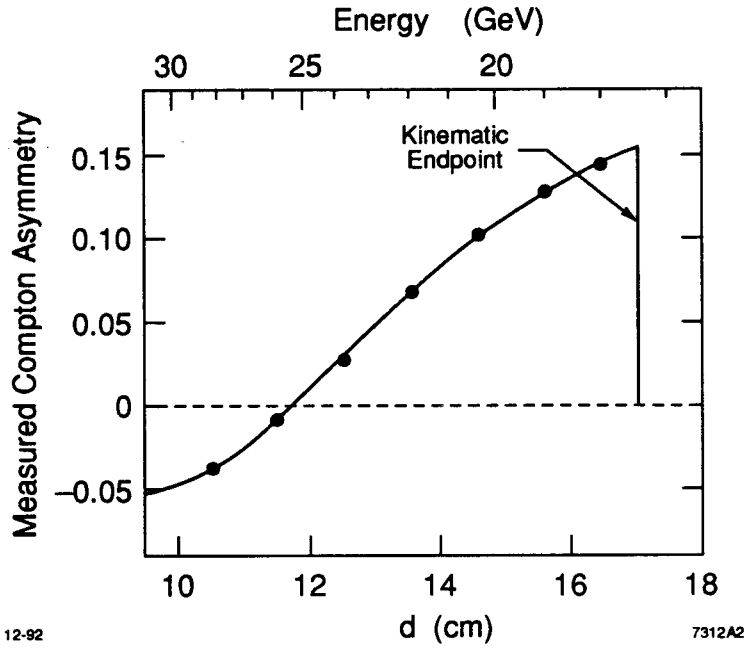

Figure 8: Measured asymmetry from Compton scattering.

Finally, the polarization of the laser, $\mathcal{P}_\gamma$, must be known to extract $\mathcal{P}_e^C$. The circular polarization of the laser is measured and routinely monitored at the laser bench and also at the analysis box just after the $e\gamma$ interaction point (CIP). (See Fig. 7.) Due to optical phase shifts in the vacuum windows entering and exiting the electron beam line at the CIP, this procedure does not automatically achieve fully circularly polarized light at the CIP itself. This was addressed about 25% of the way into the 1993 run by the addition at the laser bench of a second Pockels cell, thus allowing the production of arbitrary elliptical polarization at any point along the laser path. In particular, this guaranteed a high degree of longitudinal polarization at the CIP. For the first 25% of the data, $\mathcal{P}_\gamma$ was determined to be $(97 \pm 2\%)$, while the 75% of the data after installing the second Pockels cell gave $(99.2 \pm 0.6\%)$.

The Compton laser fires at a rate of 11 Hz. Data is acquired continuously during normal running, achieving a measurement of 0.8% statistical precision approximately every three minutes. The overall systematic error of the Compton polarization measurement is $\delta\mathcal{P}_e^C/\mathcal{P}_e^C = 1.6\%$, with the breakdown into the various contributions summarized in Table I. When this is combined with the systematic uncertainty of 1.2% in determining $\mathcal{P}_e$ from $\mathcal{P}_e^C$, as discussed in Section 2.2, the total systematic error on the polarization measurement is $\delta\mathcal{P}_e/\mathcal{P}_e = 2.0\%$.

3.2 Special Runs and Møller Polarimetry

A number of specialized SLC configurations were employed during the course of the 1993 running period to fully understand and cross-check the SLC spin dynamics and the polarization measurement. These consisted of essentially three types of procedures: Polarization measurement at the end of the Linac using Møller scattering, checks of polarization loss in the SLC North Arc, and checks of the integrity of the Compton polarization measurement. We briefly discuss the Møller and arc studies below.

A Møller scattering apparatus resides near the end of the SLC Linac in the PEP extraction line. On several occasions during the 1993 run normal data taking was interrupted and polarized electron beam was diverted to the Møller setup, where full-energy polarized SLC electrons are scattered from thin polarized iron targets. The Møller-scattered electrons are momentum selected, resulting in a narrow electron stripe whose center is determined by the Møller scattering an-

gle. A silicon strip detector following a 8.8 mm tungsten radiator measures the electron flux profile across this narrow stripe. Changing the sign of either the beam or target polarization allows one to form an asymmetry which is equal to the product of the (longitudinal) beam polarization, the target polarization, and the theoretical Møller cross-section asymmetry.

Preliminary results from the Linac Møller measurements during the 1993 run indicated values of beam polarization significantly larger than what was expected from the Compton polarimeter. However, it turns out to be essential to take into account the finite momentum of the atomic electrons of the targets. The inner-shell electrons, having larger average momentum ($\approx$ 85 KeV for the Fe K shell) contribute more to a broadening of the Møller stripe than those electrons in outer shells, such as the Fe M shell, which is where the polarized electrons reside. Hence, the measured asymmetry is affected by the finite atomic momenta. This effect, of purely kinematical origin, was noted by Levchuk,[9] and when it was incorporated[10] in our analysis, the Møller measurements agreed very well with the Compton results. The precision of the Møller measurements, limited primarily by the knowledge of the target polarization, is about 3%.

In order to quantitatively compare the Linac and IP polarization measurements, the polarization loss in the SLC arc, discussed in Section 2.2, must be included. Several special tests were performed to check the effects. The spin diffusion in the arc was checked by changing the energy spread of the beam. Beams prepared with longitudinal and transverse polarization in the Linac were transported and measured. The behavior of the spin bumps with energy was examined. The energy dependence of the measured IP polarization was well described by the models of the arc optics in all cases. The tests most directly relevant for the A_{LR} measurement were those in which the energy spread of the electron beam was made very small. In this case the spin diffusion and chromatic effects become negligibly small, and the polarization in the Linac and at the IP can be directly compared. They were found to agree well within errors. Averaged over all Møller runs, the beam polarization in the Linac was found to be $(65.9 \pm 2.1\%)$. The corresponding Compton measurements at the IP, coupled with the modelled spin losses in the beam transport, are entirely consistent with this result.

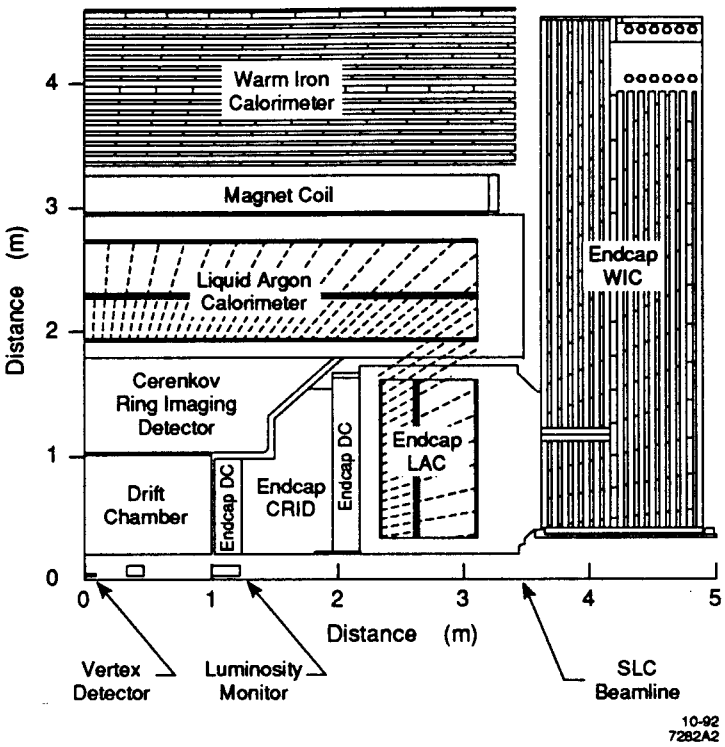

Figure 9: Quadrant view of the SLD detector.

4 Measurement of Z Events

Unlike other precision electroweak measurements involving e^+e^- at the Z resonance, A_{LR} does not rely on the detailed reconstruction of the final state. The primary requirements for SLD are a good efficiency for detection of hadronic final states which is symmetric in scattering angle, and a good separation of these events from e^+e^- final states and accelerator-related backgrounds. The measured "raw" asymmetry, A_m, defined in Eqn. 3, can then be formed.

4.1 The SLD Detector

The SLD detector is designed to fully exploit the physics of the Z in the SLC environment. A schematic of a quadrant of the detector is shown in Fig. 9. It is described in more detail elsewhere.[11] Of primary importance for the A_{LR} analysis is the SLD liquid argon calorimetry (LAC). The LAC consists of projective towers, longitudinally segmented into two electromagnetic (EM) sections of 21 radiation lengths total depth, and two hadronic sections, which combine with the EM sec-

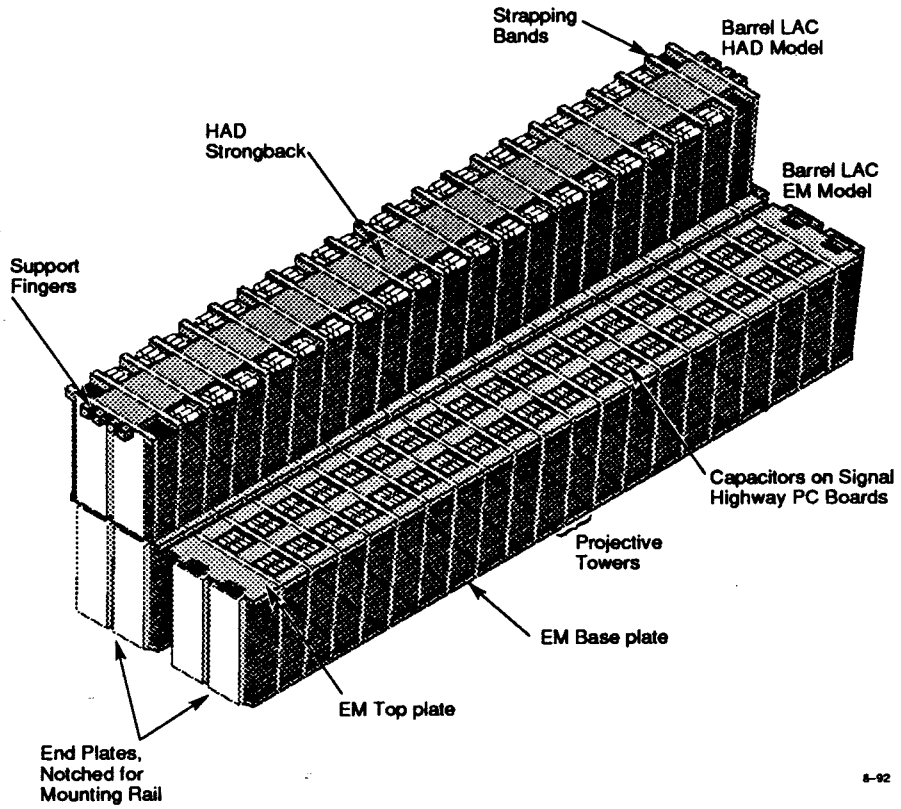

Figure 10: A module of the barrel LAC.

tions to give 2.8 interaction lengths. This is the case for both barrel and endcap sections. The LAC covers 98% of the total solid angle, with about 80% of this in the barrel section. The remainder is covered by silicon-tungsten calorimetry at small scattering angles used to measure luminosity with Bhabha scattering. Fig. 10 shows the structure of a barrel LAC module. The barrel consists of 48 such modules in azimuth and 3 along the barrel in z. There are a total of 32448 towers in the barrel and 8640 in the endcap, providing a high degree of transverse segmentation.

4.2 Event Selection

Triggers are provided on the basis of calorimetric information only, or a combination of calorimetric and charged-track information. The subsequent event selection for the A_{LR} analysis is entirely based on LAC information. Towers with at least twice the expected minimum ionizing signal were summed. Events with at

least 10 such towers adding to at least 22 GeV were retained. This reduced about 3 million triggers to about 6.4×10^4 events, which were then subjected to a full cluster reconstruction analysis. Events were required to have at least 8 clusters summing to at least 40% of the center-of-mass energy. The requirement on cluster number was primarily responsible for removing e^+e^- final states. (The predominantly t-channel e^+e^- events at small angle ($\theta \sim 50$ mrad) were separately triggered and analyzed to provide the luminosity measurement.) Accelerator-related backgrounds were largely removed by requiring that the selected events by reasonably well balanced in energy. Specifically, the energy imbalance is defined as $I = |\sum E_i \hat{r}_i| / \sum E_i$, where the sums are over clusters, each of energy E_i and unit displacement $\hat{r}_i$ relative to the IP. Events are required to have $I < 0.6$.

This procedure yielded 47,492 events. The efficiency for triggering and selecting hadronic events is ($91 \pm 1\%$), while it is 30% for $\tau^+\tau^-$ events. Muon-pair events are excluded by this procedure. The residual background fraction due to e^+e^- events and accelerator backgrounds is estimated to be $0.4 \pm 0.2\%$. Other backgrounds, due to cosmic rays or $\gamma\gamma$ events, are negligible.

5 Results and Prospects

The measured asymmetry A_m is related to A_{LR} by the following expression, an extension of that given in the Introduction, which incorporates a number of small correction terms in square brackets,

$$A_{LR} = \frac{A_m}{\langle \mathcal{P}_e \rangle} + \frac{1}{\langle \mathcal{P}_e \rangle} \left[A_m f_b - A_{\mathcal{L}} + A_m^2 A_{\mathcal{P}} - E_{cm} \frac{\sigma'(E_{cm})}{\sigma(E_{cm})} A_E - A_\varepsilon \right], \qquad (8)$$

where $\langle \mathcal{P}_e \rangle$ is the mean luminosity-weighted polarization for the 1993 run; f_b is the background fraction; $\sigma(E)$ is the unpolarized Z cross section at energy E; $\sigma'(E)$ is the derivative of the cross section with respect to E; and $A_{\mathcal{L}}$, $A_{\mathcal{P}}$, A_E, and A_ε are the left-right asymmetries of the integrated luminosity, the beam polarization, the center-of-mass energy, and the product of detector acceptance and efficiency. The individual contributions to this expression are discussed below for the 1993 run.

5.1 1993 Results

Of the 47,492 events recorded by SLD in the 1993 run, 26,195 were produced with left-hand polarized electron beam and 21,297 with right-handed beam. This gives, by Eqn. 3,

$$A_m = (10.31 \pm 0.46) \times 10^{-2} \tag{9}$$

The mean beam polarization for the run is calculated by averaging over the Compton polarimeter measurements associated with each Z event, *i.e.* the mean of the data points of Fig. 3 is formed, giving the mean $\mathcal{P}_e^C$ for the run. The correction factor for the beam chromaticity, Eqn. 6, is applied to give a preliminary result for the mean luminosity-weighted IP polarization for the run:

$$\langle \mathcal{P}_e \rangle = \frac{1}{N_Z} \sum_{i=1}^{N_Z} \mathcal{P}_i = (62.6 \pm 1.2)\% \tag{10}$$

The contributions to the error are given in Table I. The dominant error is due to the polarization measurement. The error on the chromaticity correction, Eqn. 6, also contributes to the error for this run. It should be negligible in future runs.

Table I

Systematic uncertainties that affect the A_{LR} measurement.

Systematic Uncertainty	$\delta\mathcal{P}_e^C/\mathcal{P}_e^C$ (%)	$\delta A_{LR}/A_{LR}$ (%)
Laser Polarization	1.0	
Detector Linearity	1.0	
Interchannel Consistency	0.5	
Spectrometer Calibration	0.5	
Electronic Noise Correction	0.2	
Total Polarimeter Uncertainty	1.6	1.6
Chromaticity Correction		1.2
Background Fraction (see text)		0.2
Total Systematic Uncertainty		2.0

We now discuss the contributions of the various correction factors given in Eqn. 8. The largest contribution is due to the dilution of the asymmetry from background contamination, f_b, as discussed in Section 4.2. A preliminary result for f_b is $(0.4 \pm 0.2\%)$. The uncertainty on f_b also contributes slightly to the total systematic error, and is included in Table I.

The SLC polarized electron source can produce a small left-right asymmetry in electron beam current. This would be due to a small residual component of linear polarization in the circularly polarized laser light which strikes the photocathode. The result of this could be a small left-right luminosity asymmetry, $A_{\mathcal{L}}$. This is measured in two ways. The beam current is measured by SLC toroids, and the current asymmetry is formed and associated with Z events. The pulse-by-pulse luminosity is also measured directly with a radiative Bhabha detector (RBD). The RBD is located 40 m from the IP in the North Final Focus just on the other side of the last bending magnets. Final state positrons from the process $e^+e^- \rightarrow e^+e^-\gamma$ at zero degree scattering angle will be deflected by the bend magnets into the RBD for positrons in the approximate momentum range 25–35 GeV. At peak luminosity, about 100 such positrons enter the RBD acceptance on every SLC beam crossing, thus providing a statistically precise measurement of relative luminosity or $A_{\mathcal{L}}$. Approximately midway through the run, the current of the LTR solenoid magnet was reversed, hence reversing the current asymmetry due to the polarized source, and reducing the net $A_{\mathcal{L}}$ for the run. The residual asymmetry for the run, measured with toroids and RBD, is $A_{\mathcal{L}} = (-1.0 \pm 0.2) \times 10^{-4}$.

As an additional check for a net luminosity asymmetry, the SLD small-angle Bhabha detector (LUM) directly measures luminosity, although for this application the statistical precision is limited. A total of 125,375 Bhabha events were detected in the LUM. Within the acceptance of the LUM system, the theoretically expected asymmetry is $\approx (-1.5 \times 10^{-4})\mathcal{P}_e$. The measured asymmetry is $(-32 \pm 28) \times 10^{-4}$.

The polarization and energy asymmetry factors, $A_{\mathcal{P}}$ and A_E, are directly measured and contribute negligibly small corrections. Finally, the detection asymmetry, A_ε, can be shown to be identically zero for a detector whose efficiency for detecting a final-state fermion is equal to the effieciency of detecting the anti-fermion at the same scattering angle. This is the case for a solenoidal detector such as SLD even in the presence of non-uniform detector acceptance, although

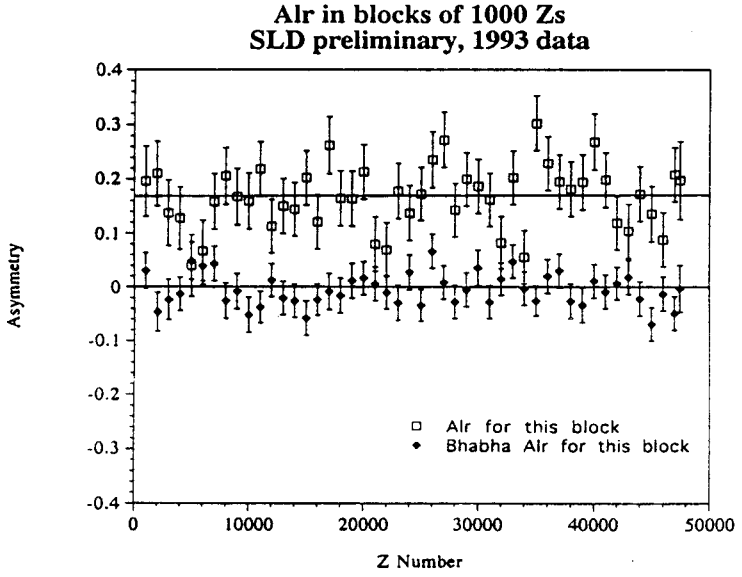

Figure 11: Left-right asymmetry for Z events (A_{LR}) and for small-angle Bhabha events in blocks of 1000 events during the 1993 run.

SLD does indeed have a very uniform acceptance.

Finally, we obtain by Eqn. 8 at $\sqrt{s} = 91.26$ GeV the preliminary 1993 result

$$A_{LR} = 0.1656 \pm 0.0073 \pm 0.0032\,, \tag{11}$$

where the first error is statistical and the second systematic, as summarized in Table I. Figure 11 shows the A_{LR} value in blocks of 1000 events over the course of the 1993 run. Also shown is the left-right asymmetry for small-angle Bhabha scattering. The coresponding preliminary 1993 weak mixing parameter is

$$\sin^2\theta_W^{\rm eff} = 0.2288 \pm 0.0009 \pm 0.0004 \tag{12}$$

This result has been corrected for the off Z-pole average center-of-mass energy and for initial state radiation. Combining this with our previous result from the 1992 run gives the preliminary value

$$\sin^2\theta_W^{\rm eff} = 0.2290 \pm 0.0010 \tag{13}$$

This result is presently the most precise single measurement of this quantity. It is somewhat smaller than the currently reported average LEP result.[12]

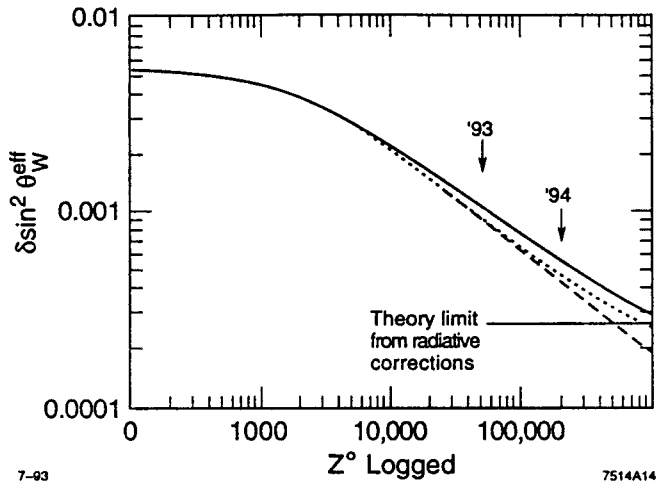

Figure 12: Error on $\sin^2\theta_W^{\rm eff}$ versus number of events for different assumptions for beam polarization and polarization measurement error. See text.

5.2 SLC Prospects and the Mega-Z Run

Figure 12 indicates how the error on $\sin^2\theta_W^{\rm eff}$ might evolve with future running. The behavior of the error can be understood from Eqn. 4 and $\delta\sin^2\theta_W^{\rm eff} \approx \delta A_{LR}/7.8$. The different curves indicate different assumptions for the value of the beam polarization and for the polarization measurement error. The solid line assumes 54% polarization and a 1% measurement error; the dashed line is 54% polarization and no measurement error; the dotted line is 58% for the first 50 K events, followed by 68% thereafter, with a 1% measurement error. The assumed polarizations are unrealistically small. Nonetheless, it is clear that the A_{LR} measurement is statistics limited, assuming a polarization measurement error of $\sim 1\%$ can be achieved. The reference to the theory limit at $\delta\sin^2\theta_W^{\rm eff} = 0.00027$ represents the present theoretical error due to uncertainty in the running of the fine structure constant, α, from low energy to M_Z. In part because of the outstanding prospects for the A_{LR} measurement, SLD has proposed a million Z ("mega-Z") program of polarized beam physics for the SLC which would take about four years to complete. We briefly discuss here the capablity of SLC/SLD to carry out this program for the A_{LR} measurement, although many other exciting physics opportunities are apparent.

Two major SLC upgrades are already in progress for the 1994 SLC run. The first is the replacement of the damping ring vacuum chambers. With the new chambers the beams will see a much smaller impedance. Bunch lengthening will

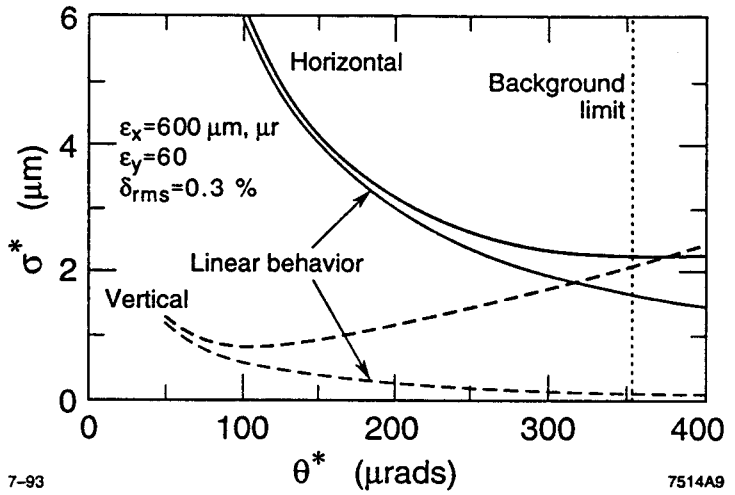

Figure 13: Calculated spot size versus angular divergence at the IP with no chromatic aberration ("Linear") and for the present Final Focus optics (unlabelled).

therefore be reduced, which is presently limiting beam current in the SLC. With the upgrade, beam pulses in excess of 4×10^{10} particles at the IP are feasible. It will also reduce beam emittance and beam energy spread. The other upgrade for 1994 is for the Final Focus optics. With ever decreasing beam emittance, the IP spot size will become completely limited by chromatic aberrations. This limitation is illustrated in Fig. 13, which is a model result[13] for IP spot size (vertical and horizontal) as a function of angular divergence (*i.e.* focussing angle) at the IP. The curves labelled "Linear" indicate the behavior in the absence of chromatic aberrations, while the unlabelled curves indicate the present Final Focus optics with chromatic aberrations included through third order. This upgrade was also assumed for Fig. 6. When these upgrades are fully exploited, the instantaneous luminosity is expected to improve by a factor of 2 to 4. In addition, the disruption enhancement factor, H_D in Eqn. 5 is calculated[14] to be $\approx$ 1.5 under these conditions.

Strained-lattice photocathodes will be incrementally improved, and those performing best on the lab bench will be chosen for SLC running. Already photocathodes yielding 80% polarization with good quantum efficiency on the bench are in hand. Therefore, it is expected, given the expected polarization losses in beam transport, that the polarization at the IP will be about 75% for the 1994 run.

The challenge of achieving a 1% polarization measurement will be met in

stages over the next two years. For the 1994 run, a new, more powerful Compton laser will be used, thus providing better signal to noise and more stable Compton measurements. In addition, the laser transport line will be upgraded in order to reduce phase shifts. Compton measurements will also be made in the Final Focus Test Beam area at the end of the Linac as a cross-check of the polarimetry and the spin diffusion in the arc. After 1994 an additional detector which measures the back-scattered Compton photons is expected to come into operation. A suitably instrumented detector would be capable of measuring the longitudinal polarization with an accuracy ($\sim 1\%$) comparable to the Cerenkov Compton electron detector, and it would also measure any transverse components of the polarization.

In summary, the prospects for achieving a high-precision measurement of $\sin^2\theta_W^{\rm eff}$ in a mega-Z SLC/SLD physics program are very good. It would represent the most precise Z asymmetry measurement, and would, along with expected improvements in the measurement of complementary electroweak parameters over the next several years, provide a non-trivial test of the Standard Model.

References

[1] K. Abe *et al.*, Phys. Rev. Lett. **70**, 2515 (1993).

[2] See for example D.C. Kennedy *et al.*, Nuc. Phys. **B321**, 83 (1989).

[3] M.L. Swartz, SLAC-PUB-4656 (1988), and references therein.

[4] ALEPH, DELPHI, L3, and OPAL Collaborations, Phys. Lett.**B276**, 247 (1992).

[5] T. Maruyama *et al.*, Phys. Rev. **B46**, 4261 1992.

[6] J. Frisch *et al.*, SLAC-PUB-6165, April 1993.

[7] T. Limberg *et al.*, Proc. 1993 Particle Accelerator Conference, Washington, D.C.; SLAC-PUB-6210, May 1993.

[8] M.J. Fero, SLAC-PUB-6026, December 1992.

[9] L.G. Levchuk, KHFTI-92-32, June 1992.

[10] M.L. Swartz *et al.*, in preparation.

[11] The SLD Design Report, SLAC Report 273, 1984.

[12] Aleph, Delphi, L3, and OPAL Collaborations, and the LEP Electroweak Working Group, CERN-PPE/93-157, August 1993.

[13] N. Walker *et al.*, Proc. 1993 Particle Accelerator Conference, Washington, D.C.

[14] P.Chen, Proc. 1993 Particle Accelerator Conference, Washington, D.C.